

FACING TARGET SPUTTER-DEPOSITED WO₃ NANOSTRUCUTRED FILMS

M. F. Hossain^{1,*}, T. Takahashi² and T. Ahmed¹

¹Department of Electrical and Electronic Engineering, Rajshahi University of Engineering & Technology (RUET),
Rajshahi-6204, Bangladesh.

²Graduate School of Science and Engineering for Reseach, Gofuku 3190, Toyama 930-8555, Japan.

*Corresponding Author : E-mail: faruk94_ruet@yahoo.com

Abstract- Nanostructured WO₃ films has been prepared on glass substrate by facing target sputtering (FTS) method with sputtering pressure, 0.1 Pa, and oxygen-annealed at 450 °C. The WO₃ films have been characterized by the Grazing incidence X-ray diffractometer (GIXRD), Field emission electron microscopy (FESEM), and Ultraviolet-visible (UV-VIS) spectrophotometer. As-deposited WO₃ film has showed amorphous structure with 13-17 nm size of nanograins. The nanostructured WO₃ films are found in annealing under oxygen environment. The whole surface is covered by WO₃ nanorods with average an diameter of 56 nm. It was revealed from optical study that the band-gap energy of WO₃ films is around 3.07 and 2.81 eV for as-deposited and annealed films, respectively.

Keywords: Tungsten oxide, facing target sputtering, nanorods, surface morphology.

1. INTRODUCTION

Tungsten oxide (WO₃) is an *n*-type semiconductor and has been investigated extensively owing to their promising physical and chemical properties [1]. WO₃ shows good optical properties and proper chemical stability; that is, *E_g* in the range of 2.5–2.8 eV (λ of 400–450 nm) is very suitable for the energy region of visible light [2, 3]. With outstanding electrochromic, optochromic, and gaschromic properties, tungsten oxides have been used to construct flat panel displays, photoelectrochromic ‘smart’ windows, optical modulation devices, wire-read-erase optical devices, catalysts [4], gas sensors [5-7] humidity and temperature sensors, and so forth [8, 9]. For the fabrication of many of such devices and increasing their efficiencies, nanostructured WO₃ films are required to be “thick and porous” enough to provide sufficient volume for producing high interaction areas. Besides, synthesis and assembly of “specific crystallographic phase” can further improve the characteristics of WO₃ [10]. The synthesis of one-dimensional (1D) nanostructures and the assembly of these nano meter-scale building blocks to form ordered superstructures or complex functional architectures offer great opportunities for exploring their novel properties and for the fabrication of nanodevices [11]. Thus for several techniques for the preparation of 1D tungsten oxide nanostructured films have been developed [1].

The deposition of WO₃ nanostructured films by facing targets sputtering technique is the newest fabrication method of thin films, with lower particle bombardment compared with the RF sputtering and DC sputtering, because of its special target arrangement. The

FTS apparatus are very effective systems for depositing high quality thin films because plasma perfectly confines by the magnetic field between two targets. The thin films can be deposited in non-bombardment by electron (“damage free”) conditions [12-14].

In this work, nanostructured WO₃ films have been deposited by using FTS method with sputtering pressure of 0.1 Pa and oxygen-annealed at 450°C. The structural, surface morphological properties of nanostructured WO₃ films have been investigated and discussed.

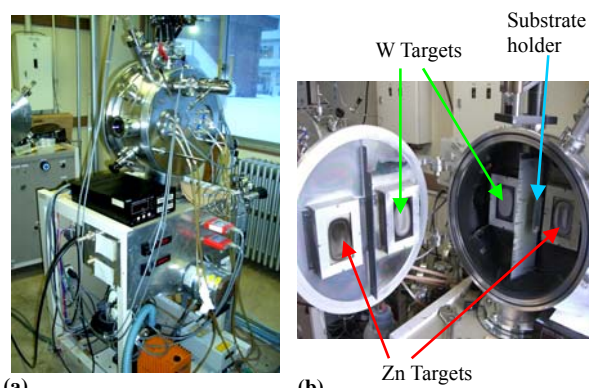


Fig. 1. Facing Target Sputtering system in our laboratory.

2. EXPERIMENTAL SECTION

Figure 1 shows the FTS systems in our laboratory for preparing WO₃ thin layer. In this FTS system, the distance between the target-to-target, and the center of the targets' to the substrate were 100 mm and 50 mm, respectively. W rectangular plates (having 115 x 75 mm, thickness of 3 mm and purity of 99.95 %) were used as

targets. The chamber was evacuated to a vacuum level of 7×10^{-4} Pa. The WO_3 nanoparticles were deposited reactively for 2hrs at DC input power of 200 W with sputtering pressure of 0.1 Pa and a fixed Ar to O_2 gas ratio (G_R) of 6:4 [15]. As-deposited WO_3 nanoparticles are annealing in a muffle furnace (TMF5, Thomas) under oxygen environment at 450°C for 2hrs, because as-deposited films are the amorphous structure. The thickness ($2 \mu\text{m}$) of the WO_3 films was determined with a mechanical surface roughness meter (SURFCOM Accretech, 1500 DX) using the step between film and substrate. The crystal structures of the TiO_2 films were determined by grazing incident X-ray diffraction (GIXRD) spectra (SHIMADZU XRD-6000) with $\text{Cu-K}\alpha$ line. The data were recorded from 2θ values 20° to 80° with a step of 0.02. For GIXRD measurement incident angle was fixed at 0.45° . The optical properties of the films were measured with JASCO V-550 spectrophotometer at room temperature within the wavelength range 300-800 nm. The surface morphologies were studied using field emission scanning electron microscope (FE-SEM) with **Model:** JEOL, FE-SEM 6700F.

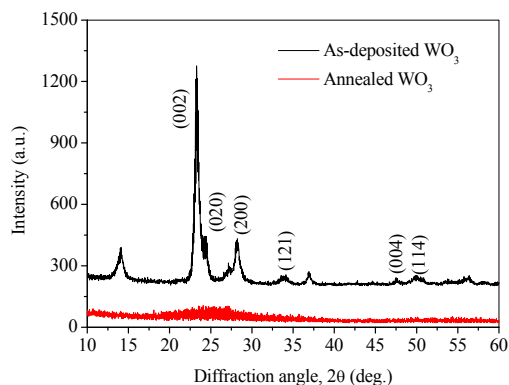


Fig.2. The GIXRD patterns of as-deposited and annealed WO_3 thin films

3. RESULTS AND DISCUSSIONS

Figure 2 shows the GIXRD patterns of as-deposited and annealed WO_3 thin film prepared on glass sample. The GIXRD patterns of the as-deposited WO_3 films are found to be amorphous in nature, but crystalline films were obtained when the film is annealed at high temperatures such as 450°C in oxygen environment. The lines located at 23.12° , 23.6° , 24.28° , 28.80° , 47.24° , and 50.52° are assigned to the lattice plane reflection of triclinic WO_3 phase with lattice parameters $a = 0.7312$ nm, $b = 0.7525$ nm, and $c = 0.7689$ nm (PC-PDF No. 83-0948). However, triclinic and monoclinic diffraction peaks almost overlap for many 2θ values and it is difficult to discriminate between these two phases. On the other hand, according to the phase diagram, the monoclinic and triclinic structures are the most common and coexist in WO_3 at temperatures lower than 500°C . [16]. The crystallite size of the particles has been estimated from the Debye–Scherrer's equation using the GIXRD line broadening as follows [17]: $D = 0.94\lambda/\beta\cos\theta$, where D is the crystallite size, λ is the wavelength of the X-ray radiation ($\text{Cu K}\alpha = 0.15406$ nm), θ is the diffraction angle and β is the FWHM. A

finite diffraction peak has been chosen for calculation of crystallite size. The diffraction peak (002) has been chosen for calculation. The derived grain size is 13.9 nm for the annealed WO_3 thin films.

Figure 3 shows the transmittance spectra as a function of wavelength (300 - 800 nm) for as-deposited and annealed WO_3 thin films, prepared in same conditions. The spectra of as-deposited WO_3 films show the usual interference pattern in the range of low absorption with a sharp fall of transmittance at the band edge. The annealed WO_3 thin film is yellowish in color. The annealed WO_3 films have less interference. It has been observed that the transmittance edge shows the red-shift with the annealed WO_3 films. It may be due to the high crystallinity, observed within the sample of investigation. The average transmittance in the visible region varies from 79% to 61% with as-deposited and annealed WO_3 films, respectively.

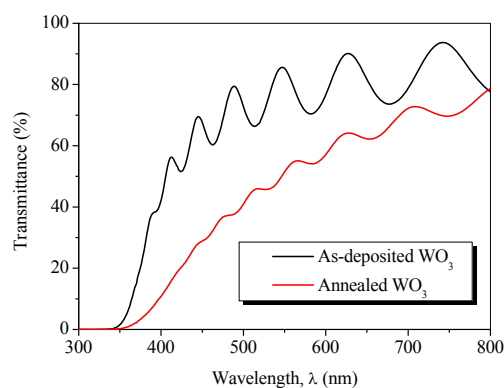


Fig.3. The optical transmittance spectra of as-deposited and annealed WO_3 thin films.

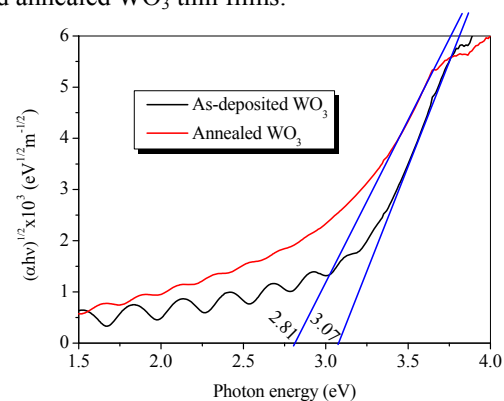


Fig.4. $(\alpha hv)^{1/2}$ versus energy for TiO_2 thin films, deposited with different sputtering powers: 200 W, 300 W, 400 W and 500 W.

We assume an indirect transition between the top of the valence band and the bottom of the conduction band in order to estimate the optical band gap (E_g) of the films using the relation [18]: $\alpha(h\nu) \propto A(h\nu - E_g)^2$, where α is absorption coefficient, A is the edge width parameter and $h\nu$ is the photon energy. Figure 3 shows the plots of $(\alpha hv)^{1/2}$ versus the photon energy of the films grown at different sputtering powers. The optical band gap of the films was determined from the extrapolation of the linear plots of $(\alpha hv)^{1/2}$ versus $h\nu$ at $\alpha = 0$. The optical band gap of the films is 3.07 and 2.81 eV for as-deposited and

annealed WO₃ films, respectively.

Figure 5 shows the surface structure and morphology of as-deposited and annealed WO₃ films. From the Fig. 5(a), the as-deposited films have a smooth surface and nanograins are observed in a larger magnification, which reaffirms their amorphous nature. The average-size of the nanograins is 13-17 nm. Annealing of the films at 450 °C not only manifests in enhancement of particle size but also in a considerably different surface morphology. It is cleared from the Fig. 5(b) that the whole surface of this film is covered by nanorods structures. The average-size of each nanorod is approximately 56 nm. After annealing the WO₃ film surface becomes rougher with an *rms* roughness of 187 nm, calculated from AFM images (not shown).

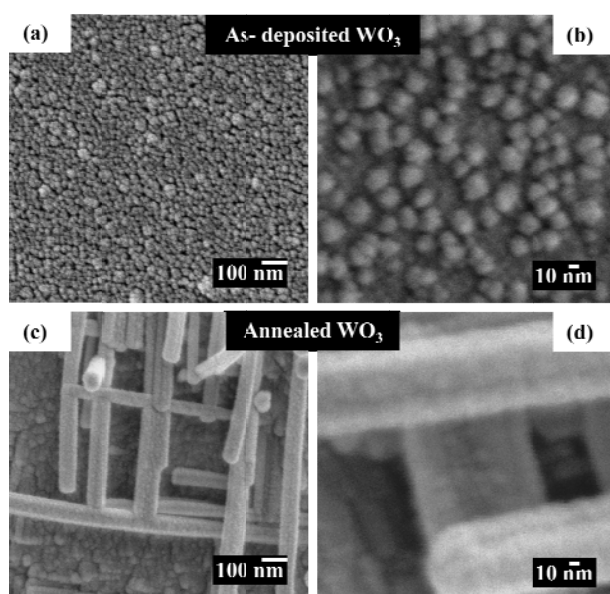


Fig. 5. FE-SEM images of as-deposited and annealed WO₃ thin films.

4. CONCLUSION

The nanostructured WO₃ films were successfully deposited on glass substrate by FTS method with sputtering pressure of 0.1 Pa and annealed at 450°C. As-deposited WO₃ films have amorphous structure and smooth surface with 13-17 nm nanograins. High crystalline film is achieved with annealed in oxygen environment. The whole surface is covered with nanorods structures. This nanostructured WO₃ films can be used for photocatalytic, electrochromic and solar cells applications. The efficiency of these devices may be enhanced by increasing the thickness of WO₃ films.

6. ACKNOWLEDGEMENT

The authors would like to thank the University of Toyama, for measurement of GIXRD, UV-VIS, FE-SEM and AFM.

7. REFERENCES

- [1] Y.B. Li, Y.S. Bando, D. Golberg, *Advanced Materials*, Vol. 15, pp 1294, 2003.
- [2] M. T. Nenadovich, T. Rajh, O. I. Micic, A. J. Nozik,

Journal of Physics and Chemistry, Vol. 88, pp. 5827, 1984.

- [3] H. P. Maruska, A. K. Ghosh, *Solar Energy*, Vol. 20, pp. 445, 1978.
- [4] F.A. Cotton, G. Wilkinson, *Advances in Organic Chemistry*, fifth ed., Wiley, New York, 1988, p. 829.
- [5] R. Boulmani, M. Bendahan, C. Lambert-Mauriat, M. Gillet, K. Aguir, Correlation between rf-sputtering parameters and WO₃ sensor response towards ozone, *Sensors and Actuators B*, Vol. 125, pp. 622-627, 2007.
- [6] M. Stankova, X. Vilanova, E. Llobet, J. Calderer, C. Bittencourt, J.J. Pireaux, X. Correig, Influence of the annealing and operating temperatures on the gassing properties of rf sputtered WO₃ thin-film sensors, *Sensors and Actuators B*, Vol. 105, pp. 271-277, 2005.
- [7] I. Jimenez, J. Arbiol, G. Dezanneau, A. Cornet, J.R. Morant, Crystalline structure, defects and gas sensor response to NO₂ and H₂S of tungsten trioxide nanopowders, *Sensors and Actuators B*, Vol. 93, pp. 475-485, 2003.
- [8] C.G. Granqvist, Electrochromic tungsten oxide films: review of progress 1993–1998, *Solar Energy Materials and Solar Cells*, Vol. 60, pp. 201-262, 2002.
- [9] K.H. Lee, Y.K. Fang, W.J. Lee, J.J. Ho, K.H. Chen, K.S. Liao, Novel electrochromic devices (ECD) of tungsten oxide (WO₃) thin film integrated with amorphous silicon germanium photodetector for hydrogen sensor, *Sensors and Actuators B*, Vol. 69, pp. 96-99, 2000.
- [10] Y.F. Guo, X. Quan, N. Lu, H.M. Zhao, S. Chen, High photocatalytic capability of self-assembled nanoporous WO₃ with preferential orientation of (0 0 2) planes, *Environmental Science & Technology* Vol. 41, Issue. 12, pp. 4422–4427, 2007.
- [11] P.X. Gao, Z.L. Wang, *Journal of Physics and Chemistry B*. Vol. 106, pp. 126533, 2002.
- [12] K. Noda, T. Kawanabe, M. Naoe. *J. Magn. Magn. Mater.* Vol. **193**, pp. 71–74, 1999.
- [13] M. Nose, T. Nagae, M. Yokota, S. Saji et al. *Surface and Coating Technology*, Vol. **116–119**, pp. 296–301, 1999.
- [14] K.H. Kim, I.H. Son, K.B. Song et al. *Applied Surface Science*, Vol. **169–170**, pp. 410–414, 2001.
- [15] M.F. Hossain, T. Takahashi, *Materials Chemistry and Physics*, Vol. 124, pp. 940, 2010.
- [16] Bittencourt, R. Landers, E. Llobet, G. Molas, X. Correig, M. A. P. Silva, J. E. Sueiras, and J. Calderer, *Journal Electrochemical Society*, Vol. **149**, pp. H81, 2002.
- [17] B.D. Cullity, *Elements of X-ray Diffraction*, Addison-Wesley, Reading, MA, USA, 1978.
- [18] J.I. Pankove, *Optical Processes in Semiconductors*, Dover Publications Inc., New York, 1970.